DATA-DRIVEN INCOMPLETELY STIRRED REACTOR NETWORK MODELING OF AN AERO-ENGINE MODEL COMBUSTOR

S. Iavarone[*], *S. Gkantonas*[*], *A. Giusti*[**], *E. Mastorakos*[*]

[*] *Department of Engineering, University of Cambridge, Cambridge, UK*

[**] *Department of Mechanical Engineering, Imperial College London, London, UK*

Abstract

Accurate predictions of soot emissions from combustion systems are required to implement the design of low-emission aero-engine combustors that can mitigate the effects of particulate matter on human health and the environment. The use of detailed models of soot formation can be unfeasible in terms of computational costs for optimisation procedures involving a large number of numerical simulations of different combustor configurations. A reduced-order formulation for turbulence-chemistry interactions and kinetic post-processing of Computational Fluid Dynamics (CFD) simulations, i.e., the Incompletely Stirred Reactors Network (ISRN) method, has recently provided promising qualitative predictions of soot emissions while allowing the use of complex chemistry at minimal computational costs. However, loss of accuracy and uncertainty in the predictions of relevant quantities, e.g., temperature and pollutant emissions, should be accounted for when reduced-order models like the ISRN method are employed. Hence, the integration of the ISRN method with data-driven approaches included in the framework of Uncertainty Quantification (UQ) has been pursued and is presented in this work. The grid parameters of the ISRN were calibrated via a UQ approach so that the predictions of temperature within an aero-engine model combustor match those obtained by a detailed CFD simulation with accuracy higher than 90%. The UQ approach results in the determination of a feasible set of grid parameters and information about the correlation between them. Then, the proposed methodology has been applied on soot emissions in the aero-engine combustor to obtain bounded predictions from the ISRN method that are of the same order of magnitude as the corresponding ones provided by the high-order Conditional Moment Closure (CMC) combustion model.

1 Introduction

The use of Computational Fluid Dynamics (CFD) tools is crucial for the development of novel, clean, and cost-effective combustion technologies. Despite the improvements in the computational capability, the implementation of detailed physics models in CFD simulations can still be challenging for sensitivity analysis and optimisation procedures, which require a large number of numerical simulations of different combustor configurations. Therefore, the implementation of reduced-order models featuring lower dimensionality and limited loss of accuracy can be beneficial. Uncertainty in the predictions of relevant quantities, such as temperature and pollutant emissions, is introduced by employing reduced-order models. This uncertainty can be, however, quantified by data-driven approaches included in the framework of Uncertainty Quantification (UQ). UQ eventually aims at minimising the uncertainty in the predictions of reduced-order models so that the latter can replicate with the highest possible accuracy the performances of the corresponding detailed models. This is achieved by calibrating important model parameters (inverse UQ) and propagating their uncertainty on the model predictions (forward UQ). Inference methods were used to perform inverse UQ and constrain the parameter space with experimental measurements in several combustion studies, such as [1, 2]. Equally numerous are the studies involving forward propagation of uncertainties to provide prediction intervals on laminar flame speeds [3, 4], ignition delay times [2, 5], and NO_x emissions [6–10].

A reduced-order formulation for turbulence-chemistry interactions and kinetic post-processing of CFD simulations, i.e., the Incompletely Stirred Reactor Network (ISRN) method, was recently presented and applied on combustors of practical interest for soot emission calculations, i.e., the Cambridge Rich-Quench-Lean (RQL) burner [11], a model aero-engine combustor [12, 13] and a single-sector model combustor operating on Jet-A1 fuel [13, 14]. The ISRN method represents a reactor network formulation of the Incompletely Stirred Reactor (ISR) theory, which is based on the Conditional Moment Closure (CMC) combustion model [15]. It provided promising results in terms of qualitative prediction of soot emissions while allowing the use of detailed chemistry at a fraction of the computational cost compared to more detailed methods. However, the sensitivity of the ISRN predictions to the network parameters has not been investigated yet. The following study presents the UQ-aided application of the ISRN approach on a model aero-engine combustor for which experimental measurements [16] and CFD simulation data [12, 13] are available. The objective of this work is to calibrate the grid parameters of the ISRN so that the predictions of temperature within the combustor replicate those obtained by the detailed CFD simulation with accuracy

higher than 90%. The UQ approach results in the determination of a feasible set of grid parameters that allow the ISRN method to reach the above-mentioned objective. The analysis also provides useful information about the correlation between the grid parameters. Subsequently, an updated feasible set of grid parameters is determined to obtain bounded predictions of soot mass fractions in the aero-engine combustor from the ISRN method that are of the same order of magnitude as the corresponding ones provided by the high-order model, i.e., the Conditional Moment Closure (CMC).

2 Methodology

The ISRN approach employed in this study is the network extension of the ISR theory developed by Mobini and Bilger [17, 18]. The ISR model can be regarded as a spatially-integrated approximation of the multi-dimensional CMC equation. An ISR is a reactive zone where the flow and the mixture fraction fields are not homogeneous but the conditional averages of the reacting scalars, conditioned on the mixture fraction, are. These assumptions grant the use of simple ordinary differential equations in mixture fraction space to model a whole combustion chamber at reduced computational costs. Details about the ISRN governing equations can be found in Refs. [11–14].

The ISRN approach is here applied on a model aero-engine combustor developed at DLR [16]. The main combustion chamber has a cross-sectional area of 0.068×0.068 m^2 and a height of 0.12 m. Ethylene is injected by sixty annular straight-channel inlets located in between two concentric nozzles introducing air with tangential velocity generated by a pair of swirlers. Additional injector ports are situated at the height of 0.08 m to radially feed secondary air into the combustion chamber, consistent with the Rich-Quench-Lean (RQL) concept. The computational domain reproducing the experimental rig is schematically shown in Fig. 1a. A single case, whose operating conditions are reported in Refs. [12, 13], is investigated.

A reference CFD simulation using Large Eddy Simulation (LES) and the CMC combustion model was performed to provide the ISRN method with the average flow fields and assess the predictive capabilities of the ISRN itself. The computational details of the LES-CMC simulation are reported in Refs. [12, 13]. The ISRN was then discretised on a coarser grid, shown in Figure 1b, which was reconstructed around the mesh of the reference LES-CMC simulation. The CFD simulation allows for arbitrary positioning of the ISRs and facilitates data transfer between solvers by exploiting the topology of the CFD faces. The grid was obtained by using two geometric series along the Z axis, parallel to the reactor centreline, and the orthogonal X and Y axes, respectively. The series have four parameters overall: the dimension dZ of the first ISR on the Z axis; the ratio rZ along the positive direction of the Z axis; the dimension dW of the same ISR on the X and Y axes; and the expansion ratio rW along the outward direction of the X and Y axes. The variability of the four grid parameters was explored via an Uncertainty Quantification (UQ) approach that aimed at determining the feasible combinations allowing the ISRN to replicate with enough accuracy the predictions of the underlying LES-CMC simulation.

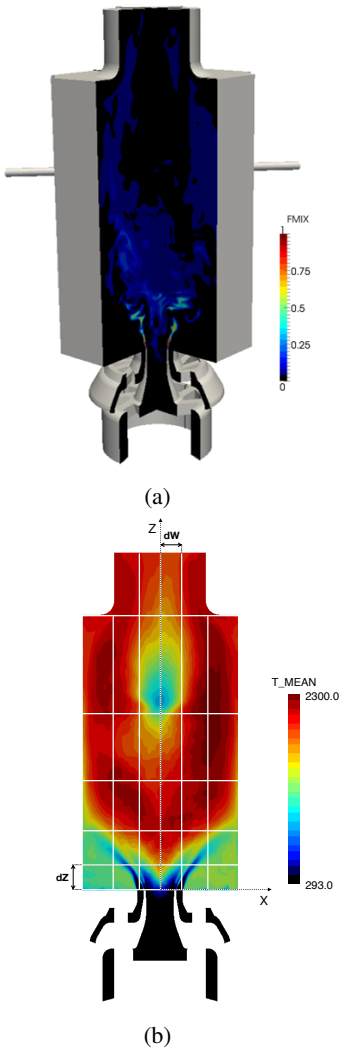

Figure 1: (a) Computational domain with instantaneous mixture fraction field, taken from Ref. [12]. (b) Contour of time-averaged temperature from the LES-CMC simulation, and representative ISRN grid depicted with white lines.

The Bound-to-Bound Data Collaboration (B2B-DC) was employed as UQ approach. Frenklach et al. [19] introduced the concept of data collaboration for the development of chemical reaction mechanisms and demonstrated that a combined analysis of several experimental datasets can increase the amount of extracted information and improve the predictions of a kinetic mechanism. Feeley et al. [20] showed that the techniques of data collaboration can be used to assess

the mutual consistency of experimental results and kinetic model predictions and identify potential outliers. From these two seminal works, B2B-DC methodology has been refined and successfully applied in several other studies [21–25]. B2B-DC lies in the deterministic UQ framework as it characterises uncertainties with interval bounds rather than probability distributions [23]. The uncertainty bounds are specified for selected quantities of interest (QoIs) and model parameters and derived from domain knowledge. The prior uncertainty region of model parameters is denoted by $\mathcal{H}$,

$$\mathcal{H} = \{\mathbf{x} \mid \alpha_k \leq x_k \leq \beta_k,\ k = 1, ..., N_p\}. \quad (1)$$

The model parameters $\mathbf{x}$ have prior uncertainty defined by lower and upper bounds α and β, respectively, which form a hyper-cube in the parameter space. The bounds affecting the QoIs are used to extract a smaller region within $\mathcal{H}$, referred to as the feasible set $\mathcal{F}$,

$$\mathcal{F} = \{\mathbf{x} \mid \mathbf{x} \in \mathcal{H},\ l_i \leq |M_i(\mathbf{x}) - d_i| \leq u_i, \\ i = 1, ..., N_{QoI}\}. \quad (2)$$

In Equation 2, $M_i(\mathbf{x})$ is the model output, which is evaluated at specified parameter inputs and compared to the corresponding datum d_i having l_i and u_i as lower and upper bounds of uncertainty, respectively. The collection of $M_i(\mathbf{x})$, d_i, l_i and u_i is referred to as a dataset. The dataset is deemed consistent if its feasible set is non-empty and inconsistent otherwise. A constrained optimisation procedure is undertaken to determine a numerical measure of consistency, indicated by C_D:

$$C_D := \underset{\mathbf{x} \in \mathcal{H}}{\text{maximise}}\ \gamma \\ \text{subject to } (1-\gamma)l_i \leq |M_i(\mathbf{x}) - d_i| \leq (1-\gamma)u_i \\ \text{for } i = 1, ..., N_{QoI}. \quad (3)$$

In Equation 3, the uncertainty affecting the datum d_i can be enlarged or reduced by the term γ. The dataset is consistent if $C_D \geq 0$, i.e., a positive maximum value of γ is obtained, proving the existence of input parameters that satisfies all the constraints. The set of data d_i in Equation 3 can come either from experiments or high-fidelity simulations. In this work, two sets of QoIs were selected: the temperature predictions and the soot mass fraction estimates of the LES-CMC simulation of the DLR burner at the centerline and at twelve horizontal cutplanes located at different heights above the inlet (from 10 to 130 mm). The data were averaged along the centerline and azimuthally averaged on the cutplanes. The prior parameter space of the ISRN model consists of the variability ranges of the four network features dZ, rZ, dW, and rW. A space-filling design was generated over the parameter space via Latin Hypercube Sampling (LHS) [26]. To explore the whole parameter space, rational-quadratic polynomials are trained on the ISRN simulation responses evaluated at the sampled points for each QoI. These polynomials act as surrogate models, namely approximation functions that are needed to emulate the behaviour of the ISRN model accurately, while being computationally cheaper to evaluate. Fifty simulations are undertaken at as many points sampled via LHS. After an adequate surrogate model is trained on simulation responses, the B2B-DC determines the feasible set of grid parameters by evaluating the consistency of 105 dataset units overall. Each unit combines the surrogate model evaluation $M_i(\mathbf{x})$, the LES-CMC prediction, either $d_i = \tilde{T}_{\text{CMC},i}$ or $d_i = \tilde{Y}_{s,\text{CMC},i}$, (where $\tilde{T}$ and $\tilde{Y}_s$ stands for averaged temperature and soot mass fraction, respectively) and the bounds l_i and u_i. The values of the bounds are determined by the level of accuracy that is required from the reduced-order model. A flow chart illustrating the steps of the methodology described above is shown in Figure 2. If the validation step is successful, i.e., the dataset is proven consistent, the workflow ends with the determination of bounded predictions from the reduced-order models with its calibrated parameters. Instead, if the dataset is inconsistent, the B2B-DC approach provides feedback to address the model-data disagreement, the bounds of variability on model parameters and data may be expanded or the reduced-order model may be improved, and the workflow in Figure 2 is continuously followed until consistency is eventually reached.

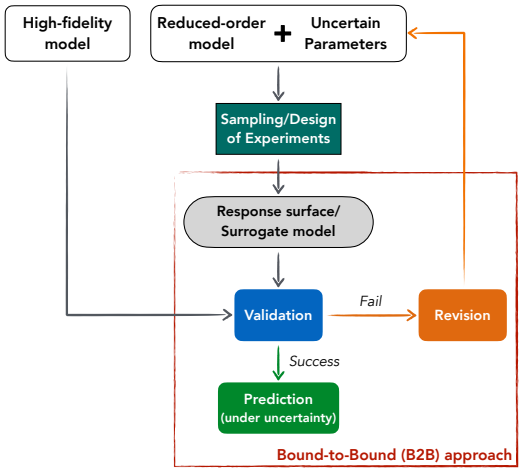

Figure 2: Methodology scheme. In this work, the high-fidelity model is the LES-CMC approach, whereas the reduced-order model is the ISRN method with its uncertain grid parameters.

3 Results and discussion

Before running the validation step of B2B-DC approach (see Figure 2 and Equation 3), the adequacy of the surrogate models must be evaluated. For each QoI, a surrogate model was trained on 80% of sampled points, whereas the remaining 20% constitutes

the test samples. The test samples were hold out from the surrogate training and used to estimate the surrogate model fitting error, via a 5-fold cross-validation [27]. The maximum error across all folds is used as the estimate of the fitting error. The maximum absolute deviation between the surrogate and the ISRN on the test points is defined as $\delta_{s,i} = \max(|S_i(\mathbf{x}_{test}) - M_i(\mathbf{x}_{test})|)$, where $S_i(\mathbf{x}_{test})$ represents the surrogate model prediction. The maximum error is propagated forward by expanding the corresponding lower and upper bounds of Equation 3, i.e., $[l_i - \delta_{s,i}, u_i + \delta_{s,i}]$. As far as temperature is concerned, the accuracy of ISRN method was fixed to a minimum of 90%. Thus, l_i and u_i are equal to $0.9d_i$ and $1.1d_i$, respectively. Figure 3 reports the histogram plot of the surrogate model fitting error for the temperature QoIs. Minimal fitting errors, below 2%, ensure the accuracy of the surrogates and the validity of the feasible set eventually provided by the B2B-DC analysis. The dataset was found

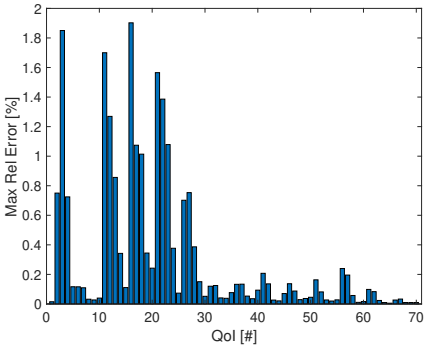

Figure 3: Histogram of the maximum relative fitting error associated with the 70 QoIs. The maximum relative fitting error reported is from the 5-fold cross-validation.

consistent as indicated by C_D = 0.0451. The feasible set of the four grid parameters was determined and is shown in Figure 4 through pair-wise projections. Figure 4 corresponds to a matrix plot, in which the diagonal sub-plots report the marginal distributions of the feasible values of the input parameters. The off-diagonal elements of the matrix plot depict the conditional distributions among the different input parameters, correlated by pairs. The axis limits of each sub-plot correspond to the initial variability ranges of the related grid parameters. From Figure 4, it can be seen that a reduction of the prior parameter space, i.e., the combined variability of the four grid parameters, was achieved.

Once the feasible set is determined, posterior bounds on the ISRN predictions for each QoI were also estimated and are shown in Figure 5. In general, a QoI prediction corresponds to solving $\left[\min_{\mathbf{x}\in\mathcal{F}} y_p(\mathbf{x}), \max_{\mathbf{x}\in\mathcal{F}} y_p(\mathbf{x})\right]$, with $\mathcal{F}$ representing the parameter feasible set and y_p the output from the surrogate model. As shown in Figure 5, the feasible parameter values allow the ISRN method to replicate the temperature predictions of the LES-CMC simulations with more than 95% accuracy at all the considered locations but the ones corresponding to QoI #11, 12, 17, 18, and 23.

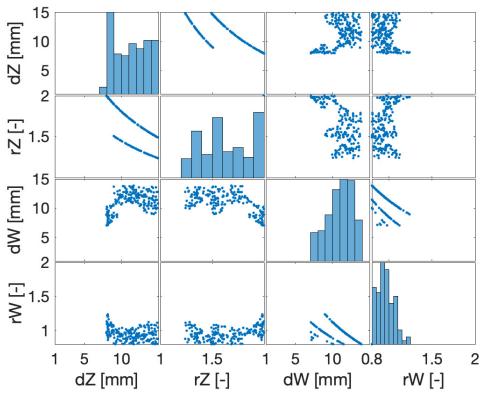

Figure 4: Pair-wise projections from the feasible set. Each scatter plot's sub-axis represents the prior bounds of the corresponding parameters.

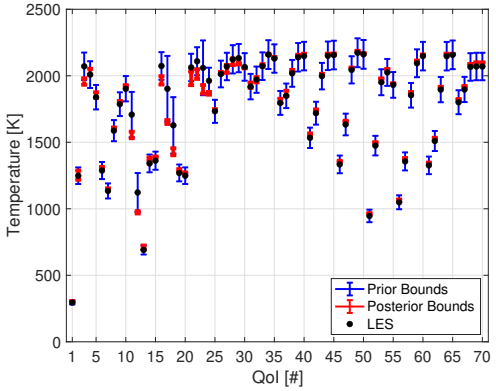

Figure 5: Comparison between the temperature predictions from the LES-CMC simulation (black dots), the prior bounds of variability matching 90% accuracy (blue bars) and the posterior bounds on the ISRN predictions (red bars).

Subsequently, additional 35 averaged values of soot mass fractions considered at 7 relevant slices were considered. Rational-quadratic surrogates were constructed on the same 50 ISRN runs for each soot mass fraction QoI. Figure 6 reports the histogram plot of the surrogate model fitting error for the soot mass fraction QoIs. The maximum fitting error is below 4%. Each fitting error is added to the initial bounds on the QOIs, as mentioned above. To reach consistency, the B2B approach was run to find the grid parameters at which the ISRN method provides soot mass fraction predictions of the same order of magnitude as the corresponding LES-CMC data. Accordingly, the lower and upper bounds l_i and u_i ascribed to the LES-CMC

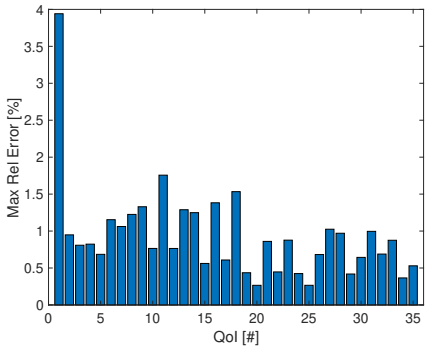

Figure 6: Histogram of the maximum relative fitting error associated with the additional 20 QoIs. The maximum relative fitting error reported is from the 5-fold cross-validation.

data were computed according to Equation 4:

$$[l_i, u_i] = [\log_{10}(d_i) - 0.5, \log_{10}(d_i) + 0.5] \quad \text{for } i = 1, ..., N_{\text{SMF}} \qquad (4)$$

where N_{SMF} is the number of soot mass fraction data taken into account as additional QoIs. The enlarged dataset was found consistent as indicated by C_D = 0.0247. The updated feasible set of the four grid parameters was therefore determined and is shown in Figure 7 through pair-wise projections. It can be noticed that a further reduction of the prior parameter space was achieved.

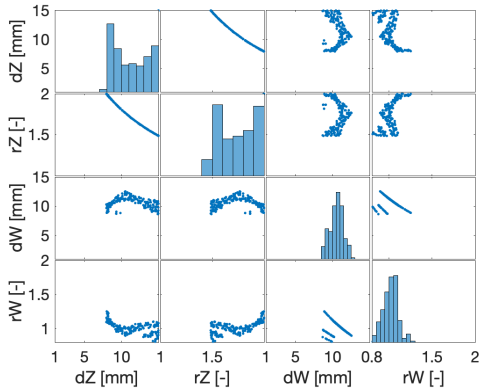

Figure 7: Pair-wise projections from the feasible set after considering 90 QoIs overall. Each scatter plot's sub-axis represents the prior bounds of the corresponding parameters.

From the updated feasible set, the reduced variability of the ISRN grid parameters was propagated through the surrogate models to obtain posterior bounds on the ISRN predictions for the additional QoIs. The posterior bounds are shown in Figure 8. Figure 8 shows that the trends provided by LES-CMC are well captured by ISRN although many posterior bounds (red bars) do not contain the corresponding LES-CMC averaged values (black points). Despite the high accuracy provided by ISRN in terms of temperature estimations, the ISRN soot predictions are not as accurate, indicating that there are sources of model inaccuracy that need to be explored and resolved. Numerical instabilities and relevant ISRN sub-models, such as for the scalar dissipation rate and the mixture fraction PDF, are being revisited. Moreover, the obtained feasible grid parameters and the corresponding number and dimensions of the ISRs must be correlated with relevant flow features as micro-mixing rates, residence times and local mixture fractions but also the gradients of conditional quantities within the domain. This analysis will assign physical meaning to the ISRN grid parameters and allow determining an optimum grid, optimised both in a numerical sense (e.g., minimisation of the sum of squared error) and a physical fashion.

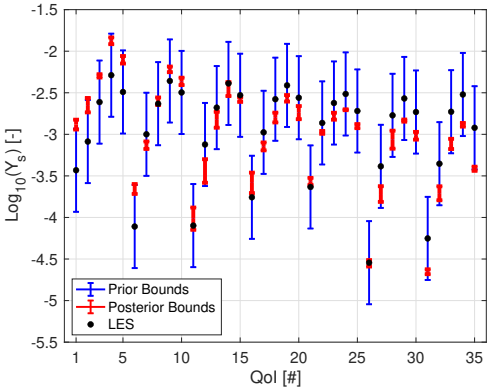

Figure 8: Comparison between the soot mass fraction predictions (shown as logarithm base 10) from the LES-CMC simulation (black dots), the prior bounds of variability matching one order of magnitude of variability (blue bars) and the posterior bounds on the ISRN predictions (red bars).

In terms of computational costs, it is essential to point out that, for this burner, the ISRN method allows reducing the runtime by two orders of magnitude compared to LES-CMC and at least an order magnitude compared to any other CFD simulation with varying level of detail, as discussed in Ref. [13]. In particular, a computation for the most refined ISRN grid (here ≈1000 ISRs) takes less than 48 hours on 128 MPI processes of an Intel Xeon Skylake supercomputer (Cambridge CSD3). Moreover, the training of 135 surrogate models takes less than 3 hours on a 4-core laptop, whereas computing the surrogate outputs is a matter of seconds on the same machine. Thus, the surrogate polynomial model used in B2B guarantees accuracy and feasibility compared to the direct use of the ISRN method for optimisation procedures.

4 Conclusions

This work reports the successful application of an Uncertainty Quantification approach to aid the modelling of an aero-engine model combustor via the Incompletely Stirred Reactor Network (ISRN) method. The calibration of the grid parameters of the ISRN has been achieved by matching with predetermined accuracy the temperature and soot mass fraction predictions of a high-fidelity CFD, i.e., LES-CMC, simulation. The initial variability of the grid parameters has been significantly reduced, and the feasible combinations allow ISRN to match with more than 90% accuracy the averaged LES-CMC temperature predictions and provide soot emissions of the same order of magnitude of the averaged LES-CMC values. The presented methodology can be seamlessly integrated with other CFD and experimental data of the DLR burner and extended to different operating conditions. Further validation of the ISRN model and the UQ approach presented in this work will be carried out on different test cases. The final goal is to validate a newly data-driven Network of Incompletely Stirred Reactor (NISeR) approach as a computationally cheaper and predictive tool that permits the use of complex soot models for estimating soot emissions, in both magnitude and trend, with a reasonable degree of accuracy.

Acknowledgements

SI acknowledges the support of the Fondation Wiener-Anspach. SG, AG and EM acknowledge the support of the UK Engineering and Physical Sciences Research Council (EPSRC) and Rolls-Royce Group. The research leading to these results has received funding from the European Union's Horizon 2020 research and innovation programme under the CoEC project, grant agreement No 952181.

References

[1] D.A. Sheen and H. Wang. *Combustion and Flame*, 158(12):2358–2374, 2011.

[2] J. Prager, H.N. Najm, K. Sargsyan, C. Safta, and W.J. Pitz. *Combustion and Flame*, 160(9):1583–1593, 2013.

[3] C. Xiouris, T. Ye, J. Jayachandran, and F.N. Egolfopoulos. *Combustion and Flame*, 163:270–283, 2016.

[4] Y. Zhang, M. Jeanson, R.. Mével, Z. Chen, and N. Chaumeix. *Combustion and Flame*, 231:111487, 2021.

[5] W. Ji, J. Wang, O. Zahm, Y.M. Marzouk, B. Yang, Z. Ren, and C.K. Law. *Combustion and Flame*, 190:146–157, 2018.

[6] A.S. Tomlin. *Reliability Engineering & System Safety*, 91(10):1219 – 1231, 2006.

[7] I. Gy. Zsély, J. Zádor, and T. Turányi. *International Journal of Chemical Kinetics*, 40(11):754–768, 2008.

[8] A.C.A. Lipardi, P. Versailles, G.M.G. Watson, G. Bourque, and J.M. Bergthorson. *Combustion and Flame*, 179:325 – 337, 2017.

[9] S. Yousefian, G. Bourque, and R.F.D. Monaghan. *Journal of Engineering for Gas Turbines and Power*, 141(10):101014, 2019.

[10] A. Durocher, P. Versailles, G. Bourque, and J.M. Bergthorson. *Combustion Science and Technology*, 192(6):959–985, 2020.

[11] S. Gkantonas, A. Giusti, and E. Mastorakos. In *Proceedings of the International Workshop on Clean Combustion: Principles and Applications*, Darmstadt, Germany, 2019. DOI:10.17863/CAM.44973.

[12] S. Gkantonas, A. Giusti, and E. Mastorakos. In *AIAA Scitech 2020 Forum*, pages 2020–2087, Orlando, Florida, 2020.

[13] S. Gkantonas. PhD thesis, University of Cambridge, 2021.

[14] S. Gkantonas, J. M. Foale, A. Giusti, and E. Mastorakos. *Journal of Engineering for Gas Turbines and Power*, 142(10):101007, September 2020.

[15] A.Y. Klimenko and R.W. Bilger. *Progress in Energy and Combustion Science*, 25(6):595–687, 1999.

[16] K.P. Geigle, R. Hadef, and W. Meier. *Journal of Engineering for Gas Turbines and Power*, 136(2), 10 2013.

[17] K. Mobini and R.W. Bilger. *Combustion Science and Technology*, 176(1):45–70, 2004.

[18] K. Mobini and R.W. Bilger. *Combustion and Flame*, 156(9):1818–1827, September 2009.

[19] M. Frenklach, A. Packard, P. Seiler, and R. Feeley. *International Journal of Chemical Kinetics*, 36(1):57–66, 2004.

[20] R. Feeley, P. Seiler, A. Packard, and M. Frenklach. *The Journal of Physical Chemistry A*, 108(44):9573–9583, 2004.

[21] P. Seiler, M. Frenklach, A. Packard, and R. Feeley. *Optimization and Engineering*, 7(4):459–478, 2006.

[22] T. Russi, A. Packard, and M. Frenklach. *Chemical Physics Letters*, 499(1):1 – 8, 2010.

[23] M. Frenklach, A. Packard, G. Garcia-Donato, R. Paulo, and J. Sacks. *SIAM/ASA Journal on Uncertainty Quantification*, 4(1):875–901, 2016.

[24] A. Hegde, W. Li, J. Oreluk, A. Packard, and M. Frenklach. *SIAM/ASA Journal on Uncertainty Quantification*, 6(2):429–456, 2018.

[25] S. Iavarone, J. Oreluk, S.T. Smith, A. Hegde, W. Li, A. Packard, M. Frenklach, P.J. Smith, F. Contino, and A. Parente. *Fuel*, 232:769 – 779, 2018.

[26] M. D. McKay, R. J. Beckman, and W. J. Conover. *Technometrics*, 21(2):239–245, 1979.

[27] P. Burman. *Biometrika*, 76(3):503–514, 1989.